BIOCHEMISTRY
including biophysical chemistry & molecular biology
Article

Biochemistry **2010,** *49,* 10535–10542 10535
DOI: 10.1021/bi101392w

Characterization of Kinetic and Thermodynamic Phases in the Prefolding Process of Bovine Pancreatic Ribonuclease A Coupled with Fast SS Formation and SS Reshuffling[†]

Kenta Arai, Fumio Kumakura, and Michio Iwaoka*

Department of Chemistry, School of Science, Tokai University, Kitakaname, Hiratsuka-shi, Kanagawa 259-1292, Japan

Received August 28, 2010; Revised Manuscript Received November 5, 2010

ABSTRACT: In the redox-coupled oxidative folding of a protein having several SS bonds, two folding phases are usually observed, corresponding to SS formation (oxidation) with generation of weakly stabilized heterogeneous structures (a chain-entropy losing phase) and the subsequent intramolecular SS rearrangement to search for the native SS linkages (a conformational folding phase). By taking advantage of DHS^{ox} as a highly strong and selective oxidant, the former SS formation phase was investigated in detail in the oxidative folding of RNase A. The folding intermediates obtained at 25 °C and pH 4.0 within 1 min (1S°−4S°) showed different profiles in the HPLC chromatograms from those of the intermediates obtained at pH 7.0 and 10.0 (1S−4S). However, upon prolonged incubation at pH 4.0 the profiles of 1S°−3S° transformed slowly to those similar to 1S−3S intermediate ensembles via intramolecular SS reshuffling, accompanying significant changes in the UV and fluorescence spectra but not in the CD spectrum. Similar conversion of the intermediates was observed by pH jump from 4.0 to 8.0, while the opposite conversion from 1S−4S was observed by addition of guanidine hydrochloride to the folding solution at pH 8.0. The results demonstrated that the preconformational folding phase coupled with SS formation can be divided into two distinct subphases, a kinetic (or stochastic) SS formation phase and a thermodynamic SS reshuffling phase. The transition from kinetically formed to thermodynamically stabilized SS intermediates would be induced by hydrophobic nucleation as well as generation of the native interactions.

Understanding of a protein folding mechanism, the process by which a protein gains its three-dimensional native structure from the random-coil state in a buffer solution, is of significant importance in relation to protein engineering (*1*, *2*) as well as various diseases caused by protein misfolded species, such as Parkinson's and Alzheimer's diseases (*3*) and amyloidosis (*4*). Remarkable experimental progress and theoretical progress have been achieved in decades in this field (*5*−*7*). Generally, two phases are presumed during the protein folding process (*8*): the first phase, which corresponds to hydrophobic nucleation from the random-coil unfolded state, and the second phase, which corresponds to conformational folding from the sterically compact state to the native state. Under redox-coupled conditions for the proteins having several disulfide (SS)[1] bonds, these phases are usually assigned to a SS formation (oxidation) process with generation of weakly stabilized heterogeneous structures (a chain-entropy losing phase) and the subsequent intramolecular SS rearrangement process to search for the native SS linkages (a conformational folding phase), respectively (*9*, *10*). By using *trans*-3,4-dihydroxyselenolane oxide (DHS^{ox}) (*11*) as a highly strong and selective oxidant, we have studied herein the former fast SS formation process in detail in the oxidative folding of bovine pancreatic ribonuclease A (RNase A) (*12*).

The SS formation in a preconformational folding process of a protein causes a significant decrease in the chain entropy, but it concomitantly results in an increase in the thermodynamic stability as reported for several model proteins, such as RNase A (*13*, *14*), lysozyme (*15*, *16*), BPTI (*17*−*19*), hirudin (*20*, *21*), etc. (*22*, *23*). In light of the conventional folding funnel model (*24*), these prefolding events take place on a slope in the rim region. The entropy loss due to SS formation shifts the unfolded state from the rim region to the center, which corresponds to the native state (N), in a horizontal direction, while the stability gain due to inter-amino acid interaction formation shifts the state in a vertical direction. If these prefolding events can be separated experimentally, the information obtained from the two individual processes would be useful for better understanding the factors that control the initial steps of protein folding.

RNase A, one of benchmark proteins in folding study, is a small monomeric protein with four native SS bonds between C26−C84, C40−C95, C65−C72, and C58−C110 (*12*). The oxidative folding pathways have been well established by Scheraga and co-workers (*25*, *26*) as shown in Figure 1. Starting from the reduced, unfolded species (R), the polypeptide chain is oxidized

[†]Supported by the Ministry of Education, Culture, Sports, Science and Technology of Japan (Grant-in-Aid for Scientific Research (B): No. 16350092). This study was also supported by fellowships to M.I. from Sumitomo Foundation and the Association for the Progress of New Chemistry of Japan.

*To whom correspondence should be addressed. E-mail: miwaoka@tokai.ac.jp. Telephone: +81 463 58 1211. Fax: +81 463 50 2094.

[1]Abbreviations: 1S, 2S, 3S, and 4S, ensembles of folding intermediates of RNase A with one, two, three, and four thermodynamically reshuffled SS linkages, respectively; 1S°, 2S°, 3S°, and 4S°, ensembles of folding intermediates of RNase A with one, two, three, and four kinetically formed SS linkages, respectively; AEMTS, 2-aminoethyl methanethiosulfonate; BPTI, bovine pancreatic trypsin inhibitor; CD, circular dichroism; DHS^{ox}, *trans*-3,4-dihydroxyselenolane oxide; DHS^{red}, reduced DHS^{ox}; DTT, dithiothreitol; DTT^{ox}, oxidized DTT; EDTA, ethylenediaminetetraacetic acid; ESI, electrospray ionization; Gdn-HCl, guanidine hydrochloride; GSSG, oxidized glutathione; HEPES, 4-(2-hydroxyethyl)-1-piperazineethanesulfonic acid; HPLC, high-performance liquid chromatography; R, reduced RNase A; RNase A, bovine pancreatic ribonuclease A; SH, thiol; SS, disulfide; Tris, tris(hydroxymethyl)-aminomathane; UV, ultraviolet.

Published on Web 11/09/2010

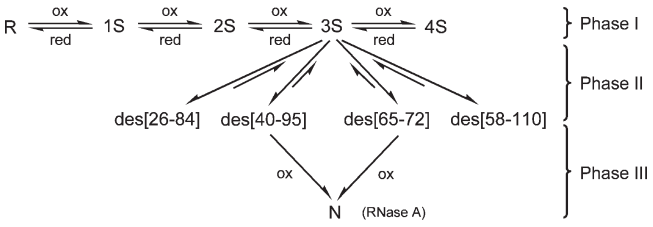

FIGURE 1: Oxidative folding pathways of RNase A. Phase I is the first SS formation phase (a chain-entropy losing phase), phase II is the second SS rearrangement phase (a conformational folding phase), and phase III is the final oxidation phase to generate the native state.

gradually to 1S, 2S, 3S, and 4S intermediates, which correspond to ensembles of the intermediate species with 1−4 SS bonds, respectively (phase I). The 3S intermediate then undergoes structural folding accompanied by slow SS rearrangement to produce des[26−84], des[40−95], des[65−72], and des[58−110] intermediates that are unique 3S intermediates having three native SS bonds but lacking one native SS bond specified (phase II). Although these key folding intermediates have native-like stable structures, only des[40−95] and des[65−72] can directly be converted to the native state (N) by oxidation with an oxidant present in the solution (phase III).

In principle, the redox-coupled folding phases, such as shown in Figure 1, could be separated by controlling the folding conditions, i.e., by selection of adequate pH, temperature, and the oxidant. However, when commonly used sulfur reagents, such as *trans*-4,5-dihydroxy-1,2-dithiane (DTT^{ox}) and oxidized glutathione (GSSG), were applied as an oxidant (*27*), clear separation between the SS formation phase (phase I) and the SS rearrangement phase (phase II) was difficult because of the narrow applicable pH range and the low oxidation ability: due to these shortcomings, oxidative folding conditions with the sulfur reagents had to be limited at slightly basic pHs and with a use of an excess amount of the oxidant, rendering the SS formation and SS rearrangement reactions to proceed competitively. In addition, under such conditions observation of the key folding intermediates, i.e., des[40−95] and des[65−72], was prevented by the rapid oxidation to N with the excess oxidant.

Recently, we have developed a new water-soluble selenium-containing oxidizing reagent DHS^{ox} (*11*) and applied it to the oxidative folding study of RNase A at 25 °C and pH 8.0 (*28*). Since DHS^{ox} is a strong oxidant, R was rapidly and quantitatively converted to 1S, 2S, 3S, and 4S sequentially without formation of any byproduct other than reduced DHS (DHS^{red}). The SS formation (oxidation) reaction was completed within 1 min, and the rate constant for each oxidation step was found to be proportional to the number of free thiol (SH) groups existing along the reactant intermediate, suggesting stochastic formation of the SS bonds. After the rapid SS formation, the SS rearrangement reaction to produce the des intermediates took place slowly via intramolecular SH−SS exchange reactions. Thus, DHS^{ox} permitted clear isolation of the SS formation phase (phase I) from the SS rearrangement phase (phase II). Another important feature of DHS^{ox} is a wide applicable pH range (at least at pH 3−9) (*29*), which would be useful to control the relative rates for the SS formation and SS reshuffling reactions involved in phase I: the SS formation corresponds to a bimolecular random oxidation process, and the SS reshuffling corresponds to an intramolecular rapid SH−SS exchange process without generation of rigid stable structures. The SS reshuffling reaction is distinctly different from the aforementioned slow SS rearrangement reaction (phase II) in that the latter accompanies generation of the native-like structures (*28*).

In the meantime, it was previously demonstrated that the major SS-bond component of the 1S and 2S intermediates isolated from the reaction mixture of reduced RNase A (R) with DTT^{ox} at 25 °C and pH 8.0 is one of the four native SS bonds, i.e., C65−C72, among 28 possible SS bonds (*30*, *31*): the population of C65−C72 was 40% in 1S and 26% in 2S. This strongly suggests that the SS formation at pH 8.0 is not fully a stochastic random process but a process producing specific SS bonds preferentially. Thus, even though no stable structure is yet formed in the 1S−4S intermediates, some thermodynamic factors, which induce a significant shift of relative populations of the SS-bond components to the native ones, must operate in the prefolding events of RNase A (i.e., phase I).

In this study, we have analyzed the prefolding events of RNase A, i.e., R → 1S → 2S → 3S → 4S coupled with SS formation, by applying DHS^{ox} as an oxidant at a variable pH from 4.0 to 10.0 and succeeded in observation of new folding subphases in the SS formation phase (phase I): the kinetic SS formation (Ia) and the thermodynamic SS reshuffling (Ib) phases. It was suggested that the prefolding intermediates obtained at pH 8.0, i.e., 1S, 2S, 3S, and 4S, are thermodynamically stabilized and have more compact structures than those obtained at pH 4.0 even though secondary and native-like rigid structures have not yet been generated.

MATERIALS AND METHODS

Materials. RNase A (type 1-A) was purchased from Sigma Aldrich Japan and used without purification. DHS^{ox} (*11*) and 2-aminoethyl methanethiosulfonate (AEMTS) (*32*) were synthesized according to the literature methods. All other reagents were commercially available and used without further purification.

Preparation of Reduced RNase A (*R*). The experimental procedure previously described (*28*) was followed. To a solution of RNase A (7−10 mg) dissolved in 0.6 mL of a 100 mM Tris-HCl/1 mM EDTA buffer solution at pH 8.5 containing 4 M guanidinium thiocyanate as a denaturant was added an excess amount of DTT^{red} (7−9 mg). The reaction mixture was incubated at room temperature for 50 min. Resulting R was purified by passing through a column packed with Sephadex G25 resin, which was equilibrated with a variable pH buffer solution purged with nitrogen: 200 mM acetate buffer, 100 mM Tris-HCl/1 mM EDTA buffer, and 25 mM $NaHCO_3$ buffer solutions were used for refolding conditions at pH 4.0, 7.0 or 8.0, and 10.0, respectively. The concentration of R was determined by UV absorbance at 275 nm based on the molar extinction coefficient (ε = 8600 M^{-1} cm^{-1} (*13*)) determined by Ellman's assay (*33*): the ε value did not change significantly in a range of pH 4.0−10.0. The R solution was immediately used in the short-term and long-term folding experiments described below.

Short-Term Folding Experiments. A quench-flow instrument (a Unisoku quench mixer equipped with a mixer controller unit) (*28*) was set up by loading the R solution, a DHS^{ox} solution in the corresponding buffer at pH 4.0, 7.0, 8.0, or 10.0, an aqueous solution of AEMTS (a SH-blocking reagent) (7 mg/mL), and a drive solution (the buffer solution at pH 4.0−10.0) in vessels A, B, C, and D, respectively. The solutions were maintained at 25.0 ± 0.1 °C by a thermostated circulating water bath system. Oxidation reaction of R was initiated by rapidly mixing 50 μL each of R and DHS^{ox} solutions. After a certain period of

time, the oxidation reaction was quenched by the reaction with 109 μL of the AEMTS solution. The reaction time was changed from 100 ms to 60 s. The obtained sample solutions were acidified at pH 3−4 by addition of 8−15 μL of 2 M acetic acid and stored at −30 °C. The dead mixing or quenching time was less than 300 ms as revealed by data fitting analysis of the relative populations of the intermediates determined by HPLC analysis.

Long-Term Folding Experiments. The R solution (200 μL) was manually added with 200 μL of the DHS^{ox} solution at pH 4.0−10.0 in a 1.5 mL microcentrifuge tube. The concentration of DHS^{ox} was regulated to be 3-fold of the concentration of R. The mixture was intensely stirred by vortexing for 5 s and was incubated for a certain period of time (1−1440 min) in a dry thermo bath regulated at 25.0 ± 0.1 °C. For the pH-jump experiment, the sample solution at pH 4.0 was added with 400 μL of 0.25 M aqueous ammonia after 5 min to increase the pH to 8.0, and the mixture was incubated at 25.0 °C for 2 min. To the resulting solution was added 200 μL of an aqueous AEMTS solution (7 mg/mL) to quench SS reshuffling and SS rearrangement reactions. The collected sample solutions were acidified to pH 3−4 with 8−15 μL of 2 M acetic acid and stored at −30 °C. Similar folding experiments were also carried out in the presence of 2−4 M guanidine hydrochloride (Gdn-HCl) at pH 8.0.

HPLC Analysis. Sample solutions from the short-term and long-term folding experiments were thawed and desalted by using a Sephadex G25 column equilibrated with 0.1 M acetic acid. The desalted solutions were analyzed by HPLC according to the method described previously (*28*). A Shimadzu VP series high-performance liquid chromatograph system equipped with a 5 mL sample solution loop and a Tosoh TSKgel SP-5PW cation-exchange 75 × 7.5 column was used. After sample injection, a Na_2SO_4 gradient was applied by linearly increasing the ratio of buffer B from 0% to 45% in 50 min at a flow rate of 0.5 mL/min: buffer A was 25 mM HEPES/1 mM EDTA at pH 7.0, and buffer B was buffer A + 0.5 M Na_2SO_4. The fractionated folding intermediates were detected by UV absorption at 280 nm. The recorded signals were integrated and analyzed by using Shimadzu LC solution software.

Characterization of Folding Intermediates. The folding intermediates (1S−4S) fractionated by HPLC were collected, purified by a Sephadex G25 column equilibrated with 0.1 M acetic acid, and lyophilized. The molecular mass of each intermediate was measured on a Jeol JMS-T100LP mass spectrometer operated in the ESI(+) mode. Since modification of the folding intermediates by AEMTS caused an increment of the molecular mass by 76 Da per the free SH group (*32*), the number of the SS bonds for each fractionated intermediate could be determined based on the observed mass number. Des[65−72] and des[40−95] intermediates were characterized unequivocally by tryptic digestion as described previously (*28*). To investigate the difference in SS-bond components of the intermediate ensembles generated at pH 4.0 and 8.0, the fractionated and lyophilized 1S intermediates that were obtained at pH 4.0 and 8.0 by the reaction of R with 1 equiv of DHS^{ox} were digested at 23 °C with trypsin for 1 h and then α-chymotrypsin for 1 h in 100 mM Tris-HCl/1 mM EDTA buffer at pH 8.0. The resulting peptide fragments were analyzed by using a Tosoh TSKgel ODS-100V reverse-phase 150 × 4.6 column (*28*).

Measurement of UV, CD, and Fluorescence Spectra. To characterize structures of the folding intermediates, the ultraviolet (UV) spectrum was recorded on a Shimadzu UV-1700 spectrophotometer by using a quartz cell (10 × 10 mm) under the conditions of 240−300 nm for the wavelength range, 30 nm/min for the scan speed, and 0.1 nm for the bandwidth. The temperature of the cell was regulated at 25.0 °C within an error of ±0.1 °C by using a circulating water bath system. Similarly, the fluorescence spectrum was measured on a Jasco FP-6200 spectrofluorometer by using a quartz cell (10 × 10 mm) under the conditions of 280 nm for the excitation wavelength, 280−400 nm for the emission wavelength range, 60 nm/min for the scan speed, 1 nm for the bandwidth, 1 s for the response, and 5 nm for the slit widths of both the excitation and emission. The same buffer solutions to those employed in the above folding experiments were used in the UV and fluorescence spectral measurement. The circular dichroism (CD) spectrum was recorded on a Jasco J-820 spectropolarimeter by using a quartz cell (10 × 10 mm) under the conditions of 260−200 nm for the wavelength range, 50 nm/min for the scan speed, 1 nm for the bandwidth, and 1 s for the response. A 10 times diluted buffer solution was used as a solvent.

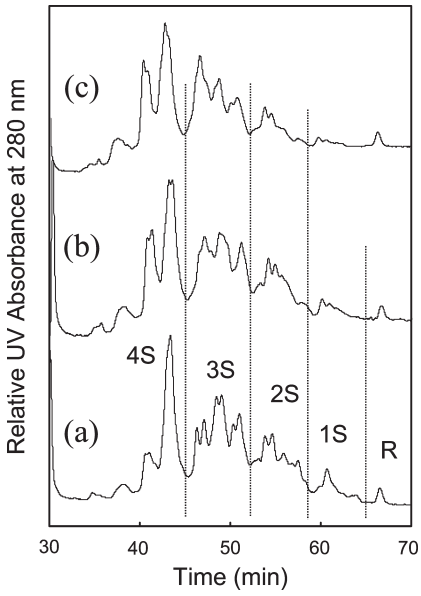

FIGURE 2: HPLC chromatograms obtained from the short-term folding experiments of RNase A using 3 equiv of DHS^{ox} as an oxidant at 25.0 °C. Reaction conditions: (a) pH = 4.0, reaction time = 50 s, $[R]_0 = [DHS^{ox}]_0/3 = 25.4$ μM; (b) pH = 7.0, reaction time = 40 s, $[R]_0 = [DHS^{ox}]_0/3 = 27.0$ μM; and (c) pH = 10.0, reaction time = 10 s, $[R]_0 = [DHS^{ox}]_0/3 = 30.2$ μM. See the text for details of the HPLC analysis conditions.

RESULTS

Short-Term Oxidative Folding of RNase A Using DHS^{ox}. Reduced RNase A with eight SH groups (R) was obtained by reduction of the native protein with DTT^{red} in the presence of a denaturant and was oxidized with stoichiometric amounts of DHS^{ox} (2−4 mol equiv with respect to R). The reaction time of the oxidation was varied from 100 ms to 60 s by using a quench-flow instrument. The free SH groups remaining in the produced folding intermediates were blocked by AEMTS to quench the intramolecular SS formation and SS reshuffling reactions: the AEMTS modification converts each SH group to $SSCH_2CH_2NH_3^+$ (*32*). Consequently, the number of SH groups, hence the number of SS bonds, of the intermediates could be easily determined according to the mass number on the mass spectrum as well as the retention time on the HPLC chromatogram by using a cation-exchange column (*13*, *28*).

Table 1: Second-Order Rate Constants for SS Formation in the Oxidative Folding of RNase A with DHS^{ox} as an Oxidant at 25 °C[a]

pH	k_1 ($mM^{-1}\cdot s^{-1}$)	k_2 ($mM^{-1}\cdot s^{-1}$)	k_3 ($mM^{-1}\cdot s^{-1}$)	k_4 ($mM^{-1}\cdot s^{-1}$)	k_{av} ($mM^{-1}\cdot s^{-1}$)[b]
4.0	7.1 ± 0.4	4.9 ± 0.3	3.0 ± 0.2	1.7 ± 0.1	1.7 ± 0.1
7.0	10.7 ± 0.5	7.3 ± 0.4	4.7 ± 0.3	2.6 ± 0.2	2.5 ± 0.2
8.0[c]	30.6 ± 0.9	20.1 ± 0.7	14.9 ± 0.8	7.4 ± 0.4	7.3 ± 0.4
10.0	42.6 ± 2.3	29.6 ± 2.3	17.9 ± 1.1	8.2 ± 0.5	9.4 ± 1.1

[a]The values of k_{1-4} were determined by fitting the data from the short-term folding experiments to the reaction scheme of eq 1. [b]The values of k_{av}, which correspond to the second-order rate constants for SS formation of peptidyl dithiol with DHS^{ox} at 25 °C, were obtained by using the equation $(k_1/4 + k_2/3 + k_3/2 + k_4)/4$. [c]Data are quoted from ref *28*.

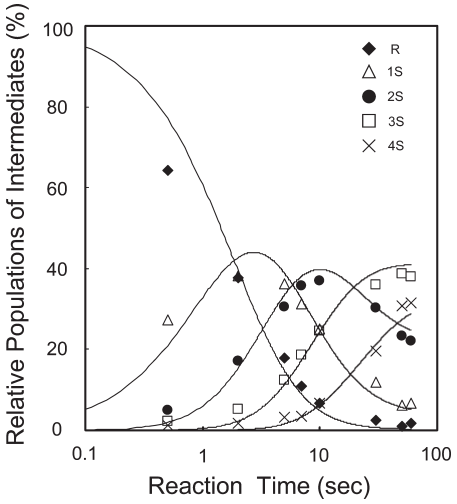

FIGURE 3: Relative populations of SS-folding intermediates as a function of the reaction time. Reaction conditions were $[R]_0 = [DHS^{ox}]_0/3 = 25.4\ \mu M$ at 25.0 °C and pH 4.0. Lines were drawn by the simulation using the second-order rate constants of $k_1 = 7.1$, $k_2 = 4.9$, $k_3 = 3.0$, and $k_4 = 1.7\ mM^{-1}\cdot s^{-1}$ based in the folding scheme of R → 1S → 2S → 3S → 4S (eq 1).

HPLC chromatograms of the folding sample solutions obtained when R was reacted with 3 equiv of DHS^{ox} at pH 4.0, 7.0, and 10.0 are shown in Figure 2. R, 1S (with one SS bond), 2S (with two SS bonds), 3S (with three SS bonds), and 4S (with four SS bonds) intermediates were separated depending on the number of the SS bonds: the least positively charged 4S eluted first, and the most positively charged R eluted last by application of a salt gradient of sodium sulfate. It is seen that 3S is a major intermediate at all pHs, indicating that SS formation reaction is completed rapidly. The reaction times required to complete the SS formation reaction were about 50, 40, and 10 s at pH 4.0, 7.0, and 10.0, respectively. This clearly shows that the velocity of SS formation by using DHS^{ox} increases with increasing the pH of the solution, in accord with the higher reactivity of a SH group at a higher pH. It should be notable that the SS formation reaction proceeded still rapidly (< 1 min) and quantitatively under an acidic condition. This is a remarkable feature of DHS^{ox} as an oxidant in application to the redox-coupled protein folding study.

Second-order rate constants k_1-k_4 for R → 1S, 1S → 2S, 2S → 3S, and 3S → 4S, respectively, at pH 4.0−10.0 (Table 1) were subsequently determined as follows. First, relative populations of the intermediate ensembles as a function of the reaction time were collected at each pH at 25 °C by integration of the HPLC chromatograms that were obtained by using 2−4 equiv of DHS^{ox}. Second, the data were fitted to the reaction scheme of eq 1. Simulation curves drawn by using the k_1-k_4 values obtained at pH 4.0 are shown in Figure 3 along with the plots of the experimental data. Good agreement between the simulation and the experiments was obtained for all conditions applied, confirming accuracy of the fitting results as well as the postulated reaction scheme (eq 1).

$$R \xrightarrow[k_1]{DHS^{ox}\ DHS^{red}} 1S \xrightarrow[k_2]{DHS^{ox}\ DHS^{red}} 2S \xrightarrow[k_3]{DHS^{ox}\ DHS^{red}} 3S \xrightarrow[k_4]{DHS^{ox}\ DHS^{red}} 4S \qquad (1)$$

The k_1-k_4 values shown in Table 1 clearly demonstrate that the higher the pH value, the larger the rate constants. The second-order rate constants averaged for the SS formation reaction with DHS^{ox} were 1.7, 2.5, 7.3, and 9.4 $mM^{-1}\cdot s^{-1}$ at pH 4.0, 7.0, 8.0, and 10.0, respectively. The rapid increase was observed in a narrow pH range between 7.0 and 8.0, which is remarkably lower than the pK_a values for cysteinyl SH groups (pK_a = 8−9) (*34*). It is also notable that the ratio of the rate constants (k_1:k_2:k_3:k_4) is roughly 4:3:2:1 at all pHs, being proportional to the number of SH groups existing in the reactant intermediates.

Long-Term Oxidative Folding of RNase A Using DHS^{ox}. After rapid cross-linking of the cysteinyl SH groups (< 1 min), an intramolecular exchange reaction between the SS bonds and the remaining free SH groups would take place in the produced folding intermediates except for 4S. Two kinds of such SH−SS exchange reactions are possible (*28*). One is the fast intramolecular exchange without generation of stable structures (called SS reshuffling). The other is the slow exchange coupled with conformational folding to produce key folding intermediates with native-like structures (called SS rearrangement). Both reactions should proceed faster at a higher pH because the SH group becomes more reactive under basic conditions.

Figure 4 shows the HPLC chromatograms of the sample solutions obtained by long-term folding experiments, where R was reacted with 3 equiv of DHS^{ox} at pH 4.0−10.0 and 25 °C. At pH 7.0 and 10.0, metastable folding intermediates, des[65−72] and des[40−95], were clearly observed in addition to native RNase A (N). Similar reactions were previously reported at pH 8.0 (*28*), where it was proposed that N is formed from the des intermediates through the slow intermolecular SH−SS exchange reaction with 1S−4S intermediates and/or possible air oxidation. The relative amount of N demonstrated that the intermolecular SH−SS exchange reaction would also proceed faster at a higher pH. At pH 4.0, on the other hand, generation of the des intermediates as well as N was not observed, indicating that the SS rearrangement can proceed efficiently only at pH 7.0 or higher: details of the conformational folding phase (phase II) observed in the long-term folding experiments will be analyzed elsewhere.

It is notable that the peak profiles for the 1S, 2S, and 3S intermediate ensembles have slowly altered at pH 4.0 during the long-term experiment for 24 h. Figure 5 shows the CD, UV, and fluorescence spectra observed at pH 4.0 in the long-term

experiments along with those for R and N for comparison. When R was reacted with 3 equiv of DHS^{ox} at pH 4.0 for 5 min, a mixture of the 1S−4S intermediates as shown in Figure 2a should be generated. The CD spectrum at this stage did not exhibit any significant differences from that of R, indicating that no secondary structure is present in the intermediates (Figure 5a). In the UV spectrum, on the other hand, the absorption around 280 nm was significantly enhanced by the reaction (Figure 5b), suggesting structural changes of the intermediates during the SS formation process. Similarly, the fluorescence spectrum exhibited an obvious decrease in the intensity around 310 nm (Figure 5c). According to these UV and fluorescence spectral behaviors, it can be delineated that during the SS formation process at pH 4.0 structures of the intermediates become compact, probably due to a chain-entropy loss, although neither secondary structure nor stable native structure is generated yet.

The spectra obtained at pH 4.0 after 24 h exhibited slightly more enhanced changes, except for CD, suggesting that structures of the folding intermediates would become more compact during the long-term incubation. Implications of the observed structural changes in the prefolding events are discussed in the next section.

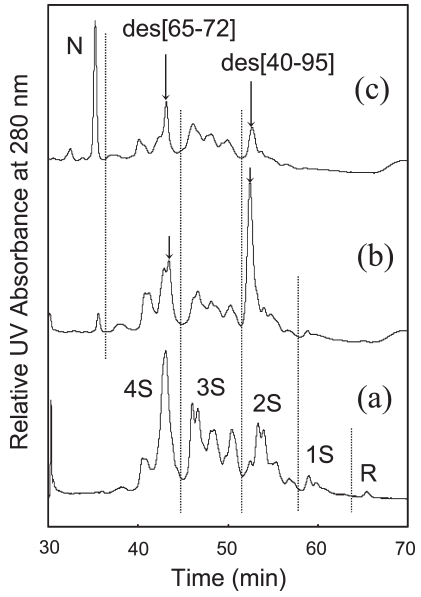

FIGURE 4: HPLC chromatograms obtained from the long-term folding experiments of RNase A using 3 equiv of DHS^{ox} as an oxidant at 25.0 °C. Reaction conditions: (a) pH = 4.0, reaction time = 24 h, $[R]_0 = [DHS^{ox}]_0/3 = 4.9\ \mu M$; (b) pH = 7.0, reaction time = 5 h, $[R]_0 = [DHS^{ox}]_0/3 = 29.1\ \mu M$; and (c) pH = 10.0, reaction time = 2 h, $[R]_0 = [DHS^{ox}]_0/3 = 20.5\ \mu M$. See the text for details of the HPLC analysis conditions.

DISCUSSION

An Applicable pH Range of DHS^{ox}. Redox-coupled oxidative folding experiments can be performed usually under limited pH conditions, i.e., at pH 8−9 around the pK_a value of a cysteinyl SH group (*34*). This is because conventional sulfur-containing oxidants, such as GSSG and DTT^{ox}, have low oxidation ability to produce a SS bond from two cysteinyl SH groups existing along a polypeptide chain (*35*). On the other hand, an applicable pH range of selenoxide DHS^{ox} was previously demonstrated to be at least from 3 to 9 (*29*). Moreover, it was recently revealed that DHS^{ox} is involved as an active intermediate in the SS formation reaction, catalyzed by the corresponding selenide (DHS^{red}), of various thiol substrates with H_2O_2 under various solvent conditions (*36*). Thus, a use of the selenoxide reagent would expand a possible solvent range for oxidative protein folding study and, therefore, will provide more general information about the folding pathways. In the present study, DHS^{ox} was applied to the oxidative folding of RNase A as an oxidizing reagent at pH 4.0−10.0. The results from short-term (~60 s) and long-term (~24 h) folding experiments have confirmed that an applicable pH range of DHS^{ox} is up to pH 10.0 at 25 °C.

Control of the Relative Reaction Rates for SS Formation and SS Reshuffling. It was clearly seen in Figure 2 that the peak profiles of the HPLC chromatogram for 1S−4S intermediate ensembles at pH 4.0 are obviously different from those generated at pH 10.0, whereas the peak profiles at pH 7.0 look similar to those at pH 10.0. The observations indicate that relative populations of the individual intermediates among the each SS intermediate ensemble are significantly different under acidic conditions from those under neutral and basic conditions. Scheraga and co-workers previously reported that when R was oxidized with DTT^{ox} at pH 8.0 and 25 °C, C65−C72 is obtained as a major SS-bond

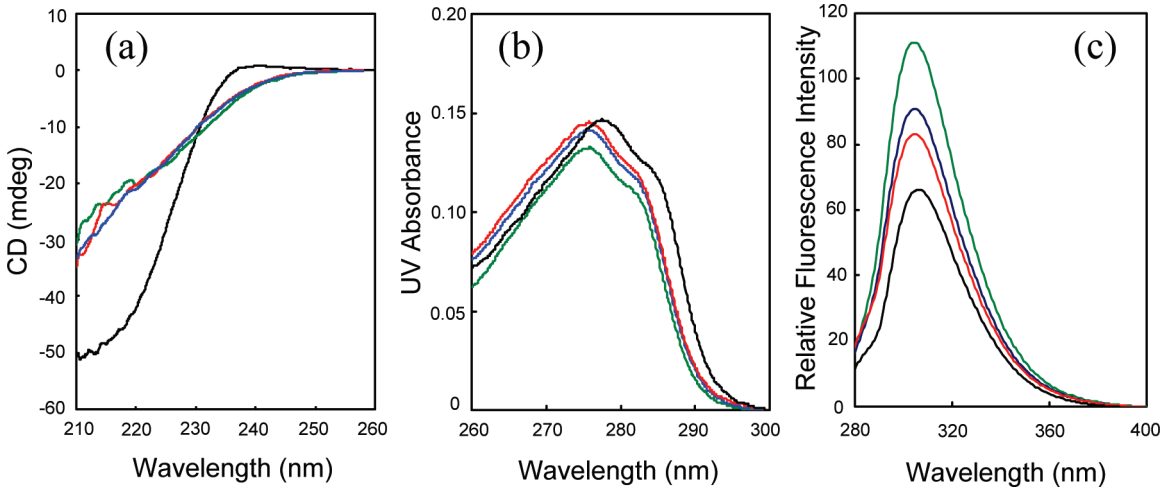

FIGURE 5: CD, UV, and fluorescence spectra observed in the long-term folding experiments of RNase A at 25.0 °C and pH 4.0. The reaction times were 5 min (blue lines) and 24 h (red lines). The respective spectra for reduced RNase A (R, green lines) and native RNase A (N, black lines) are shown for comparison. (a) CD spectra at $[R]_0 = [DHS^{ox}]_0/3 = 4.9\ \mu M$, (b) UV spectra at $[R]_0 = [DHS^{ox}]_0/3 = 15.7\ \mu M$, and (c) fluorescence spectra at $[R]_0 = [DHS^{ox}]_0/3 = 12.8\ \mu M$.

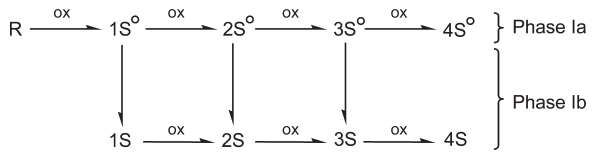

FIGURE 6: A reaction scheme of folding subphases in the prefolding SS formation phase of RNase A (phase I). Phase Ia is the kinetic (or stochastic) SS formation phase, and phase Ib is the thermodynamic SS reshuffling phase. 1S°−4S° are the kinetic folding intermediates having 1−4 SS bonds, respectively, that are generated by stochastic SS formation and are transformed to the thermodynamic folding intermediates via intramolecular SS reshuffling.

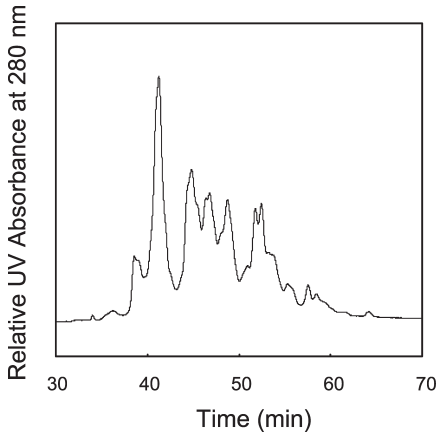

FIGURE 7: An HPLC chromatogram obtained from the pH-jump experiment of RNase A at 25.0 °C. Reaction conditions were $[R]_0 = [DHS^{ox}]_0/3 = 18.3\,\mu M$. The pH was rapidly increased from 4.0 to 8.0. See the text for details of the pH-jump and HPLC analysis conditions.

component in the 1S and 2S ensembles (*30*, *31*). This strongly suggests the possibility that the kinetically formed intermediates immediately follow transition to the thermodynamic intermediates through the rapid SS reshuffling reaction under weakly basic conditions. A possible reaction scheme of the prefolding process is shown in Figure 6, where 1S°, 2S°, 3S°, and 4S° stand for kinetically formed folding intermediates.

To obtain a direct evidence for the transition from kinetic to thermodynamic intermediates, the pH of the folding buffer solution was increased rapidly from pH 4.0 to pH 8.0 by addition of aqueous ammonia. Figure 7 shows the HPLC chromatogram obtained after the pH jump. It is seen that the peak profiles for the SS intermediates (Figure 2a) have rapidly altered to those observed at pH 7.0 (Figure 2b), except for 4S that does not have a free SH group to exchange the SS bonds. The result can be rationalized by assumption that the 1S−4S intermediates obtained at pH 4.0 are the ensembles kinetically formed (phase Ia) and they transform at neutral or basic pHs to new intermediate ensembles, which are stabilized by some thermodynamic factors (phase Ib). Indeed, when the 1S intermediate ensembles obtained at pH 4.0 and 8.0 were digested by trypsin and α-chymotrypsin, it was found that the SS-bond components at pH 4.0 are significantly different from those at pH 8.0 (see Supporting Information): especially, the population of C65−C72 was 2.5-fold increased at pH 8.0 in agreement with the previous report (*30*).

In SS-coupled folding of proteins, the prefolding process involves two fundamental reactions, i.e., SS formation and SS reshuffling. When DHS^{ox} was employed at pH 4.0, the SS formation reaction would proceed preferentially because a thiol species (SH), which is almost inert against the SS reshuffling reaction, is dominant under acidic conditions (i.e., SS formation ≫ SS reshuffling), whereas both the SS formation and SS reshuffling would proceed at pH 8.0 and 10.0 because of the presence of a reactive thiolate species (S^-) (i.e., SS formation < SS reshuffling). At pH 7.0, which is more than one unit lower than the pK_a value for the cysteinyl SH group (*34*), the SS formation and SS reshuffling would compete (i.e., SS formation ∼ SS reshuffling) as suggested by slight differences in the peak profiles at pH 7.0 and 10.0 (Figure 2). Thus, the relative rates of SS formation and SS reshuffling reactions can be controlled by changing the pH of the solution when DHS^{ox} is employed as an oxidative folding reagent. This in turn allows us to observe the kinetic SS formation phase (phase Ia) and the thermodynamic SS reshuffling phase (phase Ib) clearly separated.

Events of the Kinetic Phase (*Phase Ia*). According to the ratio of the second-order rate constants obtained at pH 4.0 (Table 1) as well as the CD spectrum observed when R was reacted with 3 equiv of DHS^{ox} at pH 4.0 (Figure 5a), it is clear that there is no stable structure in the kinetically formed folding intermediates (i.e., 1S°, 2S°, 3S°, and 4S°), although a recent time-resolved fluorescence energy transfer study coupled with a rapid-mixing continuous flow methodology suggested the presence of a densely packed core in the C-terminus of R (*37*): such a structure should be too weak to resist against an access of DHS^{ox} to the polypeptide chain. However, the concurrent changes observed in the UV and fluorescence spectra, which probe structural environments surrounding the tyrosine residues (*38*), indicated that global structures of the kinetic intermediates are significantly compact compared to R. The spectral changes obviously reflect the chain entropy loss due to SS formation. It is, therefore, conceivable that phase Ia is merely a stochastic SS formation process, which makes a conformational space of the polypeptide chain to search for the native structure considerably limited but produces no stable structure.

Events of the Thermodynamic Phase (*Phase Ib*). Intramolecular SS reshuffling was blocked at pH 4.0, but it was triggered by the pH jump to 8.0 (Figure 7). Strictly speaking, the SS reshuffling would proceed even at pH 4.0 as evidenced by the change observed in the HPLC chromatogram after 24 h (Figure 4a). Nevertheless, the change was so sluggish that the thermodynamic phase (i.e., phase Ib) coupled with the SS reshuffling could be essentially isolated from the kinetic phase (i.e., phase Ia) by using DHS^{ox}. It should be noted that the transition of phase Ib was not yet completed at pH 4.0 even after 24 h based on the difference in the peak profiles of the HPLC chromatograms between Figure 4a and Figure 2c.

The UV and fluorescence spectra obtained at pH 4.0 after 24 h (Figure 5bc) revealed that structures of the folding intermediates become slightly more compact on the average during slow SS reshuffling, suggesting existence of some thermodynamic factors that control the transition (i.e., phase Ib) from the kinetic (1S°, 2S°, 3S°, and 4S°) to the thermodynamic (1S, 2S, 3S, and 4S) intermediates. In spite of operation of the thermodynamic factors, ratios 4:3:2:1 of the rate constants k_{1-4} determined at pH 7.0−10.0 (Table 1) clearly indicated that no stable rigid structure has been generated yet in phase Ib because the presence of such structures should modify the ratio. This is in agreement with the results from previous folding experiments of RNase A at pH 8.0 using DTT as a redox couple (*14*). Further information was obtained from the oxidative folding experiment by using 3 equiv of DHS^{ox} at pH 8.0 in the presence of guanidine hydrochloride (2 M Gdn-HCl). Figure 8 shows the obtained HPLC chromatogram. Peak profiles for the intermediate ensembles were significantly different from those obtained at neutral and basic pHs in the absence of the denaturant (Figure 2bc) and rather similar to

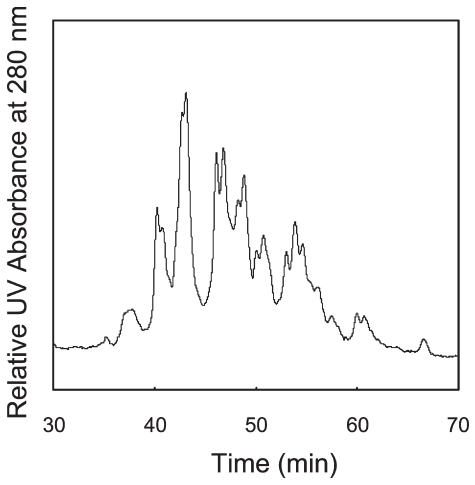

FIGURE 8: An HPLC chromatogram obtained from the long-term folding experiment of RNase A at pH 8.0 and 25.0 °C in the presence of 2 M Gdn-HCl. Reaction conditions were $[R]_0 = [DHS^{ox}]_0/3 = 4.7\ \mu M$ and reaction time = 1 min. See the text for details of the HPLC analysis conditions.

those obtained at pH 4.0 in the long-term folding experiment (Figure 4a). The result suggests that there are some structures after phase Ib but they are destroyed to some extent by the denaturant.

The events during thermodynamic phase Ib should also involve preferential formation of the C65−C72 SS bond as discussed earlier (*30*, *31*). Indeed, when R was oxidized with 6 equiv of DHS^{ox}, native RNase A (N) was not detected at pH 4.0 on the HPLC chromatogram, whereas a small portion of N (ca. 2%) was generated in 1 min at pH 8.0 (see Supporting Information Figure S9). Thus, the SS reshuffling in phase Ib would induce a shift of the SS-bond components in a direction to the native SS linkages, suggesting that the native interactions begin to generate during phase Ib.

Considering the experimental evidence discussed above, we propose that the structures generated in phase Ib are very loose hydrophobic clusters stabilized by some native interactions. Similar hydrophobic nucleation in the early folding intermediates has been evidenced for other SS-containing proteins, such as lysozyme (*39*), BPTI (*40*), and hirudin (*20*).

Implications for the SS-Intact Folding. The SS-intact unfolding and refolding processes of RNase A have been elaborately studied by several research groups (*41*−*43*). When the refolding was initiated by dilution of the reaction solution containing the SS-intact unfolded species and a denaturant, a burst folding phase could be observed in a submillisecond time scale (*44*). This phase was under debate (*45*), but a recent study has clarified that the burst phase corresponds to hydrophobic nucleation (or hydrophobic clustering) rather than a structural shift between the heterogeneous unfolded species (*43*). After the burst phase, conformational folding to the native state (N) proceeds through parallel pathways. At least four unfolded states (U_{vf}, U_f, U_m, and U_s) can be observed, and they are well characterized in relation to the conformational heterogeneity. In particular, Scheraga's group (*44*) analyzed the processes extensively and assigned each unfolded state (U) to a cis−trans conformational isomer with respect to the four X−proline (Pro) peptide bonds. In the U state, the X−Pro peptide bonds are in equilibrium, and only 2% adopts the correct native configurations (i.e., the two in trans and the other two in cis), which makes a very fast folding phase (U_{vf}).

The state after phase Ia in the SS-coupled folding of RNase A (i.e., 1S°−4S°) would be conformationally similar to the SS-intact unfolded state of RNase A in the presence of a denaturant even though the SS-bond components are significantly different. This consideration is based on the fact that no secondary structure exists in the 1S°−4S° intermediates as evidenced by the CD spectrum (Figure 5a) and a ratio of the kinetic rate constants (Table 1). However, a recent study by Chang (*46*) indicated that even at a high concentration of a denaturant some structural clusters may persist in a SS-intact unfolded state of a protein. Therefore, the 1S°−4S° intermediates may represent the fully denatured SS-intact unfolded state that cannot be attained practically under SS-intact folding conditions. The observation that the profile of the HPLC chromatogram obtained in the SS-coupled folding at pH 8.0 in the presence of 2 M Gdn-HCl (Figure 8) was not the same to that obtained at pH 4.0 in 50 s (Figure 2a) would be due to partial reservation of such hydrophobic clusters in the presence of the denaturant. It should be noted that the chromatogram shown in Figure 8 did not obviously change even in the presence of 4 M Gdn-HCl.

On the other hand, the state after phase Ib would conformationally correspond to the state obtained after the burst phase in the SS-intact folding of RNase A. Coincidence in the populations of N generated in 1 min at pH 8.0 in the short-term experiment using 6 equiv of DHS^{ox} (2%) and U_{vf} in the SS-intact unfolded state (U) (*44*) would reflect conformational similarity between 1S−4S and U. Since the presence of hydrophobic clusters with some native interactions in U has been well demonstrated (*47*), hydrophobic nucleation and accumulation of native interactions, which should significantly facilitate the subsequent conformational folding process, would be common features for the burst phase in the SS-intact folding and the SS reshuffling phase (phase Ib) in the SS-coupled folding of RNase A.

CONCLUSIONS

We have studied a preconformational folding process of the SS-coupled folding of RNase A by using DHS^{ox} as a highly strong and selective oxidant at pH 4.0−10.0 and succeeded in characterization of the kinetic SS-formation and thermodynamic SS-reshuffling subphases (phases Ia and Ib, respectively). The 1S°−4S° intermediates obtained at pH 4.0 were assigned to the intermediate ensembles with stochastically formed SS linkages. On the other hand, the 1S−4S intermediates obtained at neutral and basic pHs would be the intermediate ensembles that are stabilized by some thermodynamic factors. As a ratio of the rate constants (k_1:k_2:k_3:k_4) was roughly 4:3:2:1 at pH 4.0−10.0, being proportional to the number of SH groups along the reactant intermediates, the 1S−4S intermediates should have no rigid structure. However, the UV and fluorescence spectral changes observed during the long-term folding at pH 4.0 (Figure 5) and the HPLC chromatogram obtained from the oxidative folding at pH 8.0 in the presence of a denaturant (Figure 8) suggested that the SS reshuffling in phase Ib induces hydrophobic nucleation, which would simultaneously shift the SS-bond components significantly to the native ones on the basis of the previously revealed 1S and 2S components (*30*, *31*). Indeed, the native state (N) was included in the 4S intermediate ensemble obtained at pH 8.0 in 2% yield, whereas it was not found in the 4S° intermediate ensemble obtained at pH 4.0. Thus, the state after phase Ib should fold more easily than the state before the phase due probably to more restriction of the conformational space as well as more abundance of the native interactions.

Consequently, the prefolding SS formation process of RNase A (phase I) is not only the process to lose the chain entropy but

also the process to gain thermodynamic stability. In light of a conventional folding funnel model (*24*), the present study also suggests the possibility that the shape of the funnel in the rim region can be modified almost flat by changing the solution pH because the horizontal (i.e., the chain-entropy) process and the vertical (i.e., the energy) process at the very early stage of protein folding, though they normally proceed concertedly, were observed sequentially at an acidic pH by using a strong oxidant.

SUPPORTING INFORMATION AVAILABLE

Relative populations of SS-folding intermediates as a function of the reaction time under various conditions, HPLC chromatograms of 4S° and 4S obtained at pH 4.0 and 8.0, respectively, and LC-MS chromatograms of the peptide fragments obtained from 1S° and 1S by tryptic and chymotryptic digestion. This material is available free of charge via the Internet at http://pubs.acs.org.

REFERENCES

1. Saven, J. G. (2001) Designing protein energy landscapes. *Chem. Rev. 101*, 3113–3130.
2. Baltzer, L., Nilsson, H., and Nilsson, J. (2001) De novo design of proteins—What are the rules? *Chem. Rev. 101*, 3153–3163.
3. Forloni, G., Terreni, L., Bertani, I., Fogliarino, S., Invernizzi, R., Assini, A., Ribizzi, G., Negro, A., Calabrese, E., Volonté, M. A., Mariani, C., Franceschi, M., Tabaton, M., and Bertoli, A. (2002) Protein misfolding in Alzheimer's and Parkinson's disease: Genetics and molecular mechanisms. *Neurobiol. Aging 23*, 957–976.
4. Pepys, M. B. (2006) Amyloidosis. *Annu. Rev. Med. 57*, 223–241.
5. Duan, Y., and Kollman, P. A. (1998) Pathways to a protein folding intermediate observed in a 1-microsecond simulation. *Science 282*, 740–744.
6. Dyson, H. J., and Wright, P. E. (2002) Insights into the structure and dynamics of unfolded proteins from nuclear magnetic resonance. *Adv. Protein Chem. 62*, 311–340.
7. Faccioli, P., Sega, M., Pederiva, F., and Orland, H. (2006) Dominant pathways in protein folding. *Phys. Rev. Lett. 97*, 108101.
8. Dill, K. A. (1990) Dominant forces in protein folding. *Biochemistry 29*, 7133–7155.
9. Narayan, M., Welker, E., Wedemeyer, W. J., and Scheraga, H. A. (2000) Oxidative folding of proteins. *Acc. Chem. Res. 33*, 805–812.
10. Welker, E., Wedemeyer, W. J., Narayan, M., and Scheraga, H. A. (2001) Coupling of conformational folding and disulfide-bond reactions in oxidative folding of proteins. *Biochemistry 40*, 9059–9064.
11. Iwaoka, M., Takahashi, T., and Tomoda, S. (2001) Syntheses and structural characterization of water-soluble selenium reagents for the redox control of protein disulfide bonds. *Heteroatom Chem. 12*, 293–299.
12. Raines, R. T. (1998) Ribonuclease A. *Chem. Rev. 98*, 1045–1065.
13. Rothwarf, D. M., and Scheraga, H. A. (1993) Regeneration of bovine pancreatic ribonuclease A. 1. Steady-state distribution. *Biochemistry 32*, 2671–2679.
14. Rothwarf, D. M., and Scheraga, H. A. (1993) Regeneration of bovine pancreatic ribonuclease A. 2. Kinetics of regeneration. *Biochemistry 32*, 2680–2689.
15. Anderson, W. L., and Wetlaufer, D. B. (1976) The folding pathway of reduced lysozyme. *J. Biol. Chem. 251*, 3147–3153.
16. van den Berg, B., Chung, E. W., Robinson, C. V., and Dobson, C. M. (1999) Characterization of the dominant oxidative folding intermediate of hen lysozyme. *J. Mol. Biol. 290*, 781–796.
17. Creighton, T. E., and Goldenberg, D. P. (1984) Kinetic role of a metastable native-like two-disulfide species in the folding transition of bovine pancreatic trypsin inhibitor. *J. Mol. Biol. 179*, 497–526.
18. Creighton, T. E. (1990) Protein folding. *Biochem. J. 270*, 1–16.
19. Weissman, J. S., and Kim, P. S. (1991) Reexamination of the folding of BPTI: Predominance of native intermediates. *Science 253*, 1386–1393.
20. Chatrenet, B., and Chang, J.-Y. (1993) The disulfide folding pathway of hirudin elucidated by stop/go folding experiments. *J. Biol. Chem. 268*, 20988–20996.
21. Thannhauser, T. W., Rothwarf, D. M., and Scheraga, H. A. (1997) Kinetic studies of the regeneration of recombinant hirudin variant 1 with oxidized and reduced dithiothreitol. *Biochemistry 36*, 2154–2165.
22. Ewbank, J. J., and Creighton, T. E. (1993) Structural characterization of the disulfide folding intermediates of bovine α-lactalbumin. *Biochemistry 32*, 3694–3707.
23. Chang, J.-Y., Canals, F., Schindler, P., Querol, E., and Avilés, F. X. (1994) The disulfide folding pathway of potato carboxypeptidase inhibitor. *J. Biol. Chem. 269*, 22087–22094.
24. Wolynes, P. G., Onuchic, J. N., and Thirumalai, D. (1995) Navigating the folding routes. *Science 267*, 1619–1620.
25. Rothwarf, D. M., Li, Y.-J., and Scheraga, H. A. (1998) Regeneration of bovine pancreatic ribonuclease A: Identification of two nativelike three-disulfide intermediates involved in separate pathways. *Biochemistry 37*, 3760–3766.
26. Welker, E., Narayan, M., Volles, M. J., and Scheraga, H. A. (1999) Two new structured intermediates in the oxidative folding of RNase A. *FEBS Lett. 460*, 477–479.
27. Rothwarf, D. M., and Scheraga, H. A. (1993) Regeneration of bovine pancreatic ribonuclease A. 3. Dependence on the nature of the redox reagent. *Biochemistry 32*, 2690–2697.
28. Iwaoka, M., Kumakura, F., Yoneda, M., Nakahara, T., Henmi, K., Aonuma, H., Nakatani, H., and Tomoda, S. (2008) Direct observation of conformational folding coupled with disulphide rearrangement by using a water-soluble selenoxide reagent—a case of oxidative regeneration of ribonuclease A under weakly basic conditions. *J. Biochem. 144*, 121–130.
29. Iwaoka, M., and Tomoda, S. (2000) *trans*-3,4-Dihydroxy-1-selenolane oxide: A new reagent for rapid and quantitative formation of disulfide bonds in polypeptides. *Chem. Lett.* 1400–1401.
30. Xu, X., Rothwarf, D. M., and Scheraga, H. A. (1996) Nonrandom distribution of the one-disulfide intermediates in the regeneration of ribonuclease A. *Biochemistry 35*, 6406–6417.
31. Volles, M. J., Xu, X., and Scheraga, H. A. (1999) Distribution of disulfide bonds in the two-disulfide intermediates in the regeneration of bovine pancreatic ribonuclease A: Further insights into the folding process. *Biochemistry 38*, 7284–7293.
32. Bruice, T. W., and Kenyon, G. L. (1982) Novel alkyl alkanethiolsulfonate sulfhydryl reagents. Modification of derivatives of L-cysteine. *J. Protein Chem. 1*, 47–58.
33. Ellman, G. L. (1959) Tissue sulfhydryl groups. *Arch. Biochem. Biophys. 82*, 70–77.
34. Gilbert, H. F. (1990) Molecular and cellular aspects of thiol-disulfide exchange. *Adv. Enzymol. Relat. Areas Mol. Biol. 63*, 69–172.
35. Szajewski, R. P., and Whitesides, G. M. (1980) Rate constants and equilibrium constants for thiol-disulfide interchange reactions involving oxidized glutathione. *J. Am. Chem. Soc. 102*, 2011–2026.
36. Kumakura, F., Mishra, B., Priyadarsini, K. I., and Iwaoka, M. (2010) A water-soluble cyclic selenide with enhanced glutathione peroxidase-like catalytic activities. *Eur. J. Org. Chem.* 440–445.
37. Navon, A., Ittah, V., Scheraga, H. A., and Haas, E. (2002) Formation of the hydrophobic core of ribonuclease A through sequential coordinated conformational transitions. *Biochemistry 41*, 14225–14231.
38. Juminaga, D., Wedemeyer, W. J., Garduño-Júarez, R., McDonald, M. A., and Scheraga, H. A. (1997) Tyrosyl interactions in the folding and unfolding of bovine pancreatic ribonuclease A: A study of tyrosine-to-phenylalanine mutants. *Biochemistry 36*, 10131–10145.
39. Shioi, S., Imoto, T., and Ueda, T. (2004) Analysis of the early stage of the folding process of reduced lysozyme using all lysozyme variants containing a pair of cysteines. *Biochemistry 43*, 5488–5493.
40. Dadlez, M. (1997) Hydrophobic interactions accelerate early stages of the folding of BPTI. *Biochemistry 36*, 2788–2797.
41. Houry, W. A., Rothwarf, D. M., and Scheraga, H. A. (1994) A very fast phase in the refolding of disulfide-intact ribonuclease A: Implications for the refolding and unfolding pathways. *Biochemistry 33*, 2516–2530.
42. Qi, P. X., Sosnick, T. R., and Englander, S. W. (1998) The burst phase in ribonuclease A folding and solvent dependence of the unfolded state. *Nat. Struct. Biol. 5*, 882–884.
43. Kimura, T., Akiyama, S., Uzawa, T., Ishimori, K., Morishima, I., Fujisawa, T., and Takahashi, S. (2005) Specifically collapsed intermediate in the early stage of the folding of ribonuclease A. *J. Mol. Biol. 350*, 349–362.
44. Houry, W. A., and Scheraga, H. A. (1996) Nature of the unfolded state of ribonuclease A: Effect of cis-trans X-Pro peptide bond isomerization. *Biochemistry 35*, 11719–11733.
45. Krantz, B. A., Mayne, L., Rumbley, J., Englander, S. W., and Sosnick, T, R (2002) Fast and slow intermediate accumulation and the initial barrier mechanism in protein folding. *J. Mol. Biol. 324*, 359–371.
46. Chang, J.-Y. (2009) Structural heterogeneity of 6 M GdmCl-denatured protein: Implications for the mechanism of protein folding. *Biochemistry 48*, 9340–9346.
47. Welker, E., Maki, K., Shastry, M. C. R., Juminaga, D., Bhat, R., Scheraga, H. A., and Roder, H. (2004) Ultrarapid mixing experiments shed new light on the characteristics of the initial conformational ensemble during the folding of ribonuclease A. *Proc. Natl. Acad. Sci. U.S.A. 101*, 17681–17686.